# Design of Flexible Green Anti Radiation Shielding Material against Gamma-ray

**ALI BASHEER AZEEZ[1]*, KAHTAN S. MOHAMMED[1], MOHD MUSTAFA AL BAKRI ABDULLAH[1,2], NIK NORIMAN ZULKEPLI[1,2], ANDREI VICTOR SANDU[1,3]*, KAMARUDIN HUSSIN[1,2], AZMI RAHMAT[1]**

[1]Center of Excellence Geopolymer & Green Technology (CEGeoGTech), School of Materials Engineering, Universiti Malaysia Perlis (UniMAP), 01000, P.O.Box, D/A Pejabat Pos Besar, Kangar, Perlis, Malaysia

[2] Faculty of Engineering Technology (FETech), Universiti Malaysia Perlis (UniMAP), 01000, P.O.Box, D/A Pejabat Pos Besar, Kangar, Perlis, Malaysia

[3]Gheorghe Asachi Technical University of Iasi, Faculty of Materials Science and Engineering, 41A D Mangeron Blv., 700050, Iasi, Romania

*The utilization of waste rubber powder in polymer matrices provides an attractive strategy for polymer waste disposal. In this study lead free composite material samples for anti– radiation purposes were produced. To attain this goal, 15 wt. % of recycled acrylonitrile-butadiene rubber (NBRr) were added to Naturalrubber (NR) to prepare the composite's matrix part. Then the matrix was incorporated with various hard materials wastes such as iron particulates, iron fillings and slags brought from different industry zones. The amounts of the added particulates were ranged from 15–75 wt%. All fabricated samples were assessed for their anti-radiation attenuation properties. The attenuation measurements were performed using gamma spectrometer of NaI (Tl) detector. The utilized radiation sources comprised $^{137}Cs$ and $^{60}Co$ radioactive elements with photon energies of 0.662 MeV for $^{137}Cs$ and two energy levels of 1.17 and 1.33MeV for $^{60}Co$. Likewise theHalf-Value Layer (HVL) and the mean free paths (Mfp) for the tested samples were obtained. The aim of this work is to investigate the effects of the waste loading rates, the particulate types and their dispersive manner within the rubber blends on the attenuation coefficients. The maximum linear attenuation coefficient ($\mu$)was attained for rubber incorporates iron particulates wastes of 65 wt. %. They were of $0.0510\pm 3.2123 \times 10^{-3}$for $^{137}Cs$ and $0.0346\pm 6.973\times 10^{-3}$and $0.0182\pm 1.297\times 10^{-3}$ for $^{60}Co$for the energies of 0.662, 1.17and 1.33 MeV respectively. A Significant improvement of attenuation performance was achieved by 25%–30% for rubber samples incorporate iron particulate. The tested samples were examined using different techniques, metallographic facilities, optical microscopy, scanning electron microscopy (SEM), Fourier Transform Infrared (FTIR) Spectroscopy, and hardness and measurement facilities. The microstructure, homogeneity, particulate dispersion, porosity and structure defects, and the mechanical properties of the fabricated samples were studied and evaluated.*

*Keywords: Attenuation coefficient, radioactive, wastes iron filings, NR/NBRr blends, SEM, NaI (Tl), steel slag*

In recent years, the practice of recycling has been encouraged and promoted by increasing awareness in environmental matters and the subsequent desire to save resources. The relatively high cost of polymers and sometimes high levels of scrap material generated during manufacturing make recycling viable and attractive option [1].

Recycled latex has become a focus of attention compared with reclaimed rubber due to the lightly cross linked and high quality nature of rubber hydrocarbon [2].

Day by day radiation protection becomes more and more important topic to be investigated in nuclear science. Shielding from gamma rays is more difficult than others because gamma photons have no mass and charge and hold high-energy, they can readily penetrate into the matter [3].

For long time lead was used for anti radiation protection whether alone or within concrete walls in radiology departments to protect both workers and patients from any unnecessary exposure to ionizing radiation [4-6].

Over the past years a great deal of concern has been expressed about the toxicity of lead [7]. Human lead toxicity in children as well as adults is well documented [8-14].There are also reports on the need for corrective measures due to corrosion of lead sheets when lead is used for structural shielding [15].

These shocking facts steered researchers to look for alternative anti radiation materials. Other materials such as steel in paraffin/poly-ethylene, hydrogen, silicon or carbon, boron and depleted uranium were proposed for anti radiation protection [16–18].

These materials are not easy to be processed, relatively expensive and not abundant; some others are expected to cause cancer like depleted uranium.

Based on the above mentioned facts, production of cheap environment friendly non-toxic lead-free radiation shields which provide less weight compared to conventional lead-based shields remains a challenging issue in radiation protection.

In composite materials, a single number cannot represent the atomic number as in the case of an element. This number is defined as the "effective atomic number" and it is a convenient parameter for evaluation of photon interaction with the medium [19].

Gamma rays and radioactive radiations are widely used in nuclear stations, radiotherapy industry and hospitals to serve a wide range of commercial purposes. However, if not handled carefully, high intensity gamma radiations can

* *email: alibasheer2013@yahoo.com, sav@tuiasi.ro*

cause skin burn, birth defects, organ damage cancer hair loss and even death (depending on the exposure and intensity of the rays) [20]. Among a number of protective measures against gamma radiations, one of the most effective is applying protective shields. A radiation shield, as the name implies, serves the purpose of creating strong barrier between high intensify gamma particles and external environment [21].

On commercial scale the effectiveness of a radioactive protection shield is measured in terms of HVL (half value layer) and TVL (tenth value layer). Common materials used in protection shields are lead, rubber and iron whose standard TVL and HVL values are well known [22- 25].

A number of research studies have focused on the ways through which the shielding properties of rubber can be improved. However, very few researches have proposed the idea of mixing metal ores and aggregates with rubbers to enhance the flexibility, absorbing and shielding properties of rubber [26, 27].

In a research Maheemeed et al. [28] determined and compared the coefficient of linear attention of five different compositions of rubber-lead samples. The composition and ingredient ratio of every sample was different from each other. From the findings it was concluded that HVL and energy of the sample was found to be inversely proportional to each other. On the other hand mixing ratios and μ were found to be directly proportional to each other.

In another research study Aghamiri M.R. et al. [29] investigated the properties of a number of metals and ores which are considered effective against radioactive radiations. In this study the code which was used to figure the attenuation of x-ray particles was MCNP4C (Monte Carlo Code). Along with theoretical simulations, experimental tests were also conducted to determine the properties of different kinds of shields. Among a number of different meats and ores, tin and tungsten were found to the most effective ones. It was also found that a blend of tungsten and tin can serve the purpose of very strong and effective radioactive radiation shield.

Huge amounts of used materials, wastes, and by-products of NBRr, iron fillings, iron particulates and slags can be consumed in the production of these environment friendly anti-radiation human vests. Otherwise they have to be sent to the landfill. NBRr is not biodegradable; it can remain in nature for hundreds of years. Some metal wastes are hazardous and can be leached from the landfill to the drinking water by many means and threaten the life of human beings. Optimum anti radiation performance can be attained by manipulating the particulate size, distribution and orientation of the metal contents within the NR matrix [30, 31].

To assess the attenuation degree, gamma spectrometer of NaI (Tl) detector was used. The utilized radiation sources comprised $^{137}Cs$ and $^{60}Co$ radioactive elements. The μ value, the mass attenuation coefficients (μ/ρ), HVL and the Mfp were measured using computer code software.

The long range target of this study is to develop a cost effective environment friendly non-toxic lead-free anti radiation human vest of effective shielding properties based on recycled materials to be worn by workers working at the fields of warehouses for nuclear wastes and private rooms for X-ray and radiation therapy equipment in medical fields.

## Experimental part

*Materials and methods*

Raw material of genuine Natural rubber NR and recycled NBRr items such as gloves, stethoscope's tubes, milled items of acrylonitrile butadiene rubber NBRr were used to prepare the soft component (matrix) of the NR–hard particulates composite material in this study. The NR recycled items were passed through a two-roll mixing mill for a fixed time of 5 min.

Carbon black N330, N-cyclohexyl-2-benzothiazyl-sulphenamide CBS, zinc oxide, stearic acid, sulphur, and processing oil were added to the blend. Before milling, the NBRr was sieved using an Endecott sieve and particle size analysis was performed by Master sizer Instrument type E.

Then the blend was mixed with different loading rates of various metal wastes such as iron particulates in size range 800-1100 μm, iron filing and steel slags of range 100–188μm in size to produce the final NR/NBRr–hard particulates samples. The wastes loading rates i.e. the hard component in these composite material samples were ranged from 15–75 wt. %.

Three sets of NR/NBRr–hard particulates samples were prepared. Each sample was of 5mm in thickness. The NBRr particle size in each sample ranged from 500–1000 μm.

The iron particulates and the iron fillings were collected from the workshops of the school of material and the school of manufacturing engineering in Kangar and from the industrial area in Penang- Malaysia. In generals these metal wastes and debris were from mechanical turning, milling and abrasive machining operations of steel, mainly mild steel.

The steel blast furnace slags supplied by Ann Joo Resources Berhad Steel Company in Betaling Jaya Kuala Lumpur. Before usage the metal particulates were passed through degreasing, cleaning and milling. The iron particulates iron filing and the steel slags were refined and sieved to about (800-1100) μm and (100 to188) μm respectively. The characteristics of the materials used are listed in table 1.

Figure 1 shows the features of the slags and metal particulates of the samples used in this study. Figure 2 showed the grain size of the additives (a) Iron filing, (b) Iron particulate. The rubber–hard particulates admixture was mixed for 25 min which were considered enough to achieve good homogeneity.

The characteristics of the rubber and waste materials used are shown in table 1.

| Materials | Description | Source |
|---|---|---|
| Natural rubber (NR) | | Bayer (M) Ltd |
| Milled acrylonitrile butadiene rubber NBRr gloves size: | 500-1000 μm | Juara One Resources Sdn Bhd,Bukit Mertajam, Penang, Malaysia. |
| Waste materials:<br>Iron fillings size:<br>Iron particulate size:<br>Steel slags size: | <br>150-188μm<br>250-500 μm<br>150-188 μm | Industrial area in Penang<br>Industrial area in Penang<br>Ann Joo Resources Berhad Steel Company in Betaling Jaya Kuala Lumpur. |
| N-Cyclohexyl-2-benzothiazyl sulphenamide (CBS), zinc oxide, Antioxidant, stearic acid, sulphurand filler | | Anchor Chemical Co (M) Ltd |

**Table 1**
MATERIALS CHARACTERISTICS

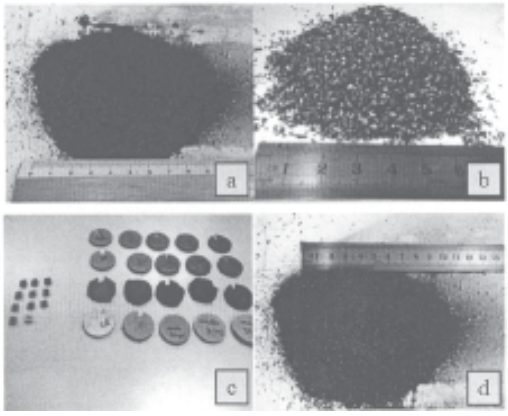


Fig. 1. Low magnification optical graphs of the materials used in this study: (**a**) steel slags crushed and screened (**b**) Iron particulates (**c**) the 5mm thickness NR/NBRr–hard particulates samples (**d**) Iron fillings.

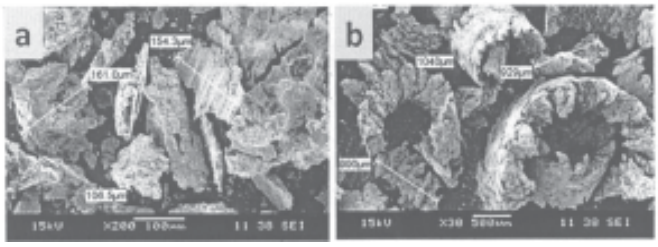


Fig. 2. The grain features of the additives
(a) Iron filing (b) Iron particulate

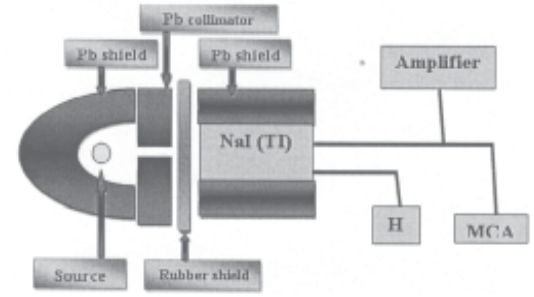


Fig. 3. Schematic representation of the experimental setup

| Compounds / Ingredients | phr | | | | |
|---|---|---|---|---|---|
| | Sample 1 | Sample 2 | Sample 3 | Sample 4 | Sample 5 |
| NR | 100 | 100 | 100 | 100 | 100 |
| NBRr | 15 | 15 | 15 | 15 | 15 |
| Zinc oxide | 5 | 5 | 5 | 5 | 5 |
| Stearic acid | 2 | 2 | 2 | 2 | 2 |
| Sulphur | 2 | 2 | 2 | 2 | 2 |
| N-Cyclohexyl-2-benzothiazole Sulphenamide(CBS) | 1 | 1 | 1 | 1 | 1 |
| Antioxidant | 1 | 1 | 1 | 1 | 1 |
| Filler | 10 | 10 | 10 | 10 | 10 |
| Additives: Iron fillings, Iron particulates and Steel slags wt. % | 15% | 25% | 45% | 65% | 75% |

**Table 2**
FORMULATION OF NR/NBRR AND ADDITIVES BLENDS

*Compounding, Cure Characteristics and Vulcanization*

The NR/NBRr blends were formulated with loading ratios of different NR recycled materials, necessary chemical additives and waste hard particulate materials as shown in table 2. The NR/NBRr materials were pre-blended and the mixing procedure was carried out at room temperature using a two-roll milling machine according to the ASTM D 3184-89 .Curing was conducted according to ASTM D 2240-93 using a Monsanto Moving Die Rheometer instrument (MDR 2000) Samples of the respective compounds of about 4g each were used for testing at vulcanization temperature of 160°C. Then the rubber compounds were compression molded at 160C° using a hot press according to the respective cure time of $t_{90.}$

*Mechanical Properties and surface morphology*

The hardness testing was performed according to ASTM D 1415-88.SEM was used to examine the surface morphology of the exposed areas of the NR/NBRr blends. The surfaces of the samples were mounted on aluminum stubs and sputter coated with a thin layer of gold about 1.5–3.0 nm thick to avoid electrostatic charging and poor resolution during examination. Three-dimensional surface scanning analyses was used to examine the porosity on the samples surface.

*Measurement of Attenuation coefficients Properties*

A MCA (Multi Channel Analyzer) along with a 3" × 3" NaI (Tl) detector was used to determine the attenuation coefficient values of gamma rays. To develop a communication link between commuter and the equipment an intelligent software program Genie200 was used.

The energy of high velocity photons emitted by two resources i.e. $^{60}Co$ and $^{137}Cs$ were found to be approximately 0.662, 1.173 and 1.332 MeV. In order to measure the accurate values of linear coefficients of given samples experimental tests using a mono-energetic narrow and intense beam of gamma rays was used. For schematic setup of the experiment (fig. 3).

*Calculations*

Calculations started with subtracting the background from the initial intensity (Io) and intensity of the beam. There is a direct relation between the mass and the density. To calculate the coefficient of linear attenuation, gamma rays were transmitted through a target on a sample, whose thickness was known. Figures 4 and 5 show the spectra of gamma rays emitted by the sources $^{60}Co$ and $^{137}Cs$. The areas under the peaks of the gamma rays will be considered to evaluate the intensity of the beam. However, to evaluate

initial intensity, the sample between the detector and the source was removed. The coefficient of linear attenuation is determined by the formula:

$$\mu = \frac{1}{x} \ln \frac{I_0}{I} \quad (1)$$

where, x = 5 mm (known thickness of samples).

In order to acquire a significantly high pulse distribution, the spectrum of gamma rays used in the experiment was obtained for a real time of about 80s.

Moreover the above equation (called the buildup factor B) is only valid when two of the following conditions are satisfied:

- the photons present in the incident beam should completely be mono-energetic;
- the incident beam should be very narrow (for intense and precise focus).

The mean free path which is defined as the average distance high speed photons cover between collisions is related to attenuation coefficient [33]. Te relation is determined by the following equation:

$$mpf = \mu^{-1} = ((\mu/\rho)\rho)^{-1} \quad (2)$$

Where; $\mu$ is the linear attenuation coefficient, $\mu/\rho$ is the mass attenuation coefficient and $\rho$ is the density of the material.

The average values of standard deviation of the synthesized sample are determined by the formula:

$$\sigma(\bar{\mu}) = \frac{\sqrt{\sum(\mu i - \bar{\mu})^2}}{N-1} \quad (3)$$

Where $\sigma(\mu)$ is the standard deviation at any position, $\mu$ is the linear attenuation coefficient at any position of the sample, $\mu$ is the average values of the linear attenuation coefficient and N is the number of the measured positions for each sample, in this study they were 8 positions.

The half layer values of the sample are determined by the following equation:

$$HVL = 0.693/\mu \quad (4)$$

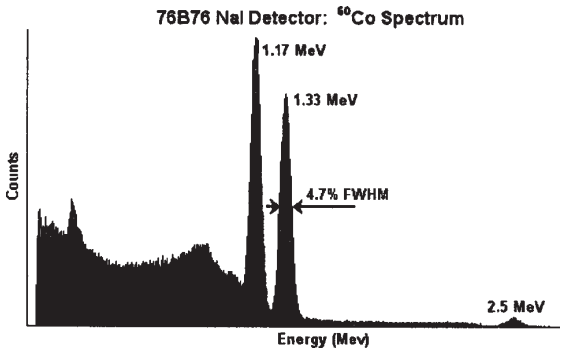


Fig. 4. Gamma ray spectrum obtained from $^{60}$Co source

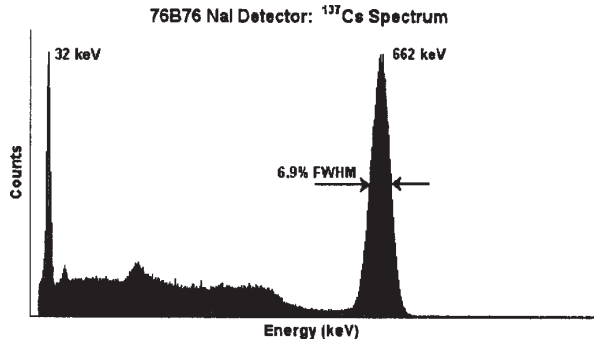


Fig. 5. Gamma ray spectrum obtained from $^{137}$Cs source

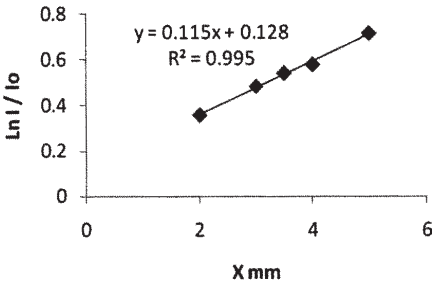


Fig. 6. Linear attenuation coefficients from the measured I and $I_o$ values as a function of the sample thickness x for the $^{137}$CS source.

Whereas HVL is the average amount of material needed to absorb 50% of all radiation, it is related to mean free path *mpf*.

Linear coefficient of attenuation is evaluated by graphical method. In this method the slope between the fixed line ln (Io/I) and transmitted radiation is determined by the formula number 1.

Figure 6 shows the plot versus thickness of the sample and total value of linear attenuation.

**Results and discussions**

There different sample of NBRr/NR with different weight ratios were tested. Each sample consists of five sub-samples of rubbers. In each rubber sample the content of waste product was gradually increased from 15 to 75 wt %. The mixture of waste products consisted of iron particulates, iron filing and steel slags brought from steel industry waste product extracted firm steel manufacturing industry. For SEM micrograph of rubber insulation with different additives, (fig. 7).

Average values of coefficient of linear attenuation, standard deviation, HVL, mean free path and extent of hardness of all the three samples, are discussed in tables 3, 4, 5. The radioactive sources of these samples were

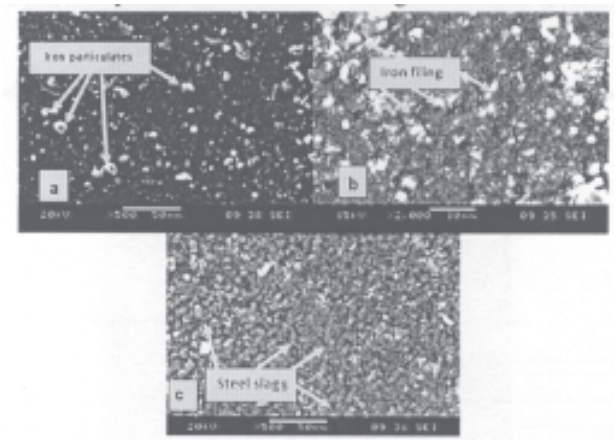


Fig. 7. Rubber matrix with different additives (a) iron particulates (b) iron filings (c) steel slags.

$^{137}$Cs and $^{60}$Co with energy levels 0.662MeV and 1.17-1.33MeV respectively.

A quick glance at these tables shows that there is very slight shift variation in the standard deviation values of these samples. This gives good indications that the fabricated samples have good homogeneity and of even distributions of the dense components within the rubber cohesive mixture.

| E(MeV) | Sets | Parameters | Sample 1 (15wt. %) | Sample 2 (25wt. %) | Sample 3 (45wt. %) | Sample 4 (65wt. %) | Sample 5 (75wt. %) |
|---|---|---|---|---|---|---|---|
| $^{137}$Cs 0.662MeV | Set1 Iron particulates | $\bar{\mu}$ (mm$^{-1}$)& $\sigma(\bar{\mu})\times10^{-3}$ | 0.0221±3.85 | 0.0281± 7.94 | 0.0301±6.34 | 0.0410± 3.2123 | 0.0343 ± 4.568 |
| | | HVL (mm) | 31.36 | 24.66 | 23.02 | 16.90 | 20.20 |
| | | Mfp (mm) | 45.24 | 35.58 | 33.22 | 19.60 | 29.15 |
| | | Hardness test | 36 | 39 | 41 | 42 | 37 |
| | Set2 Iron filling | $\bar{\mu}$ (mm$^{-1}$)& $\sigma(\bar{\mu})\times10^{-3}$ | 0.0211±6.28 | 0.0231±9.63 | 0.0281±3.19 | 0.0351±2.973 | 0.0321±6.846 |
| | | HVL (mm) | 32.85 | 30.00 | 24.66 | 19.74 | 21.29 |
| | | Mfp (mm) | 47.39 | 43.29 | 35.58 | 28.49 | 31.15 |
| | | Hardness test | 33 | 36 | 34 | 29 | 30 |
| | Set3 Steel slices | $\bar{\mu}$ (mm$^{-1}$)& $\sigma(\bar{\mu})\times10^{-3}$ | 0.0197±8.53 | 0.0201±9.24 | 0.0227±6.37 | 0.0291±6.981 | 0.0272±5.926 |
| | | HVL (mm) | 35.18 | 34.48 | 30.53 | 23.81 | 25.48 |
| | | Mfp (mm) | 50.76 | 49.75 | 44.05 | 34.36 | 36.76 |
| | | Hardness test | 40 | 43 | 46 | 50 | 55 |

**Table 3**
AVERAGE LINER ATTENUATION COEFFICIENT (mm$^{-1}$) WITH THE STANDARD DEVIATION, HVL, HARDNESS AND mfp FOR THE TESTED SAMPLES FOR $^{137}$Cs SOURCE OF 0.662MeV

| E(MeV) | Sets | Parameters | Sample 1 (15wt. %) | Sample 2 (25wt. %) | Sample 3 (45wt. %) | Sample 4 (65wt %) | Sample 5 (75wt. %) |
|---|---|---|---|---|---|---|---|
| $^{60}$Co 1.17MeV | Set1 Iron particulates | $\bar{\mu}$ (mm$^{-1}$) & $\sigma(\bar{\mu})\times10^{-3}$ | 0.01B3= 8.83 | 0.0208= 7.6B | 0.0239= 9.53 | 0.0346= 6.973 | 0.02B8= 7.841 |
| | | HVL (mm) | 37.B7 | 33.32 | 29.00 | 20.03 | 24.06 |
| | | Mfp (mm) | 54.64 | 48.07 | 41.B4 | 28.90 | 34.72 |
| | | Hardness test | 36 | 39 | 41 | 42 | 37 |
| | Set2 Iron filling | $\bar{\mu}$ (mm$^{-1}$) & $\sigma(\bar{\mu})\times10^{-3}$ | 0.0173=7.92 | 0.0178=2.9B | 0.0181=1.92 | 0.0201=4.9B2 | 0.0198=5.395 |
| | | HVL (mm) | 40.06 | 38.94 | 38.29 | 34.48 | 35.00 |
| | | Mfp (mm) | 57.80 | 56.17 | 55.24 | 49.75 | 50.50 |
| | | Hardness test | 33 | 36 | 34 | 29 | 30 |
| | Set3 Steel slices | $\bar{\mu}$ (mm$^{-1}$) & $\sigma(\bar{\mu})\times10^{-3}$ | 0.0171=3.B2 | 0.0175=4.B2 | 0.0176=B.25 | 0.01B2=3.5B1 | 0.017B=2.937 |
| | | HVL (mm) | 40.53 | 39.60 | 39.3B | 3B.0B | 3B.94 |
| | | Mfp (mm) | 5B.47 | 57.14 | 56.B1 | 54.94 | 56.17 |
| | | Hardness test | 40 | 43 | 46 | 50 | 55 |

**Table 4**
AVERAGE LINER ATTENUATION COEFFICIENT (mm$^{-1}$) WITH THE STANDARD DEVIATION, HVL, HARDNESS AND mfp FOR THE TESTED SAMPLES FOR $^{60}$Co SOURCE OF 0.662MeV

| E(MeV) | Sets | Parameters | Sample 1 (15wt. %) | Sample 2 (25wt. %) | Sample 3 (45wt. %) | Sample 4 (65wt. %) | Sample 5 (75wt. %) |
|---|---|---|---|---|---|---|---|
| $^{60}$Co 1.33MeV | Set1 Iron particulates | $\bar{\mu}$ (mm$^{-1}$) & $\sigma(\bar{\mu})\times10^{-3}$ | 0.016B=7.39 | 0.0171=6.92 | 0.0178=3.92 | 0.01B2=1.297 | 0.0170=B.643 |
| | | HVL (mm) | 41.25 | 40.53 | 3B.94 | 3B.0B | 40.77 |
| | | Mfp (mm) | 59.52 | 5B.47 | 56.17 | 54.94 | 5B.B2 |
| | | Hardness test | 36 | 39 | 41 | 42 | 37 |
| | Set2 Iron filling | $\bar{\mu}$ (mm$^{-1}$) & $\sigma(\bar{\mu})\times10^{-3}$ | 0.0170=5.7B | 0.0169=2.9B | 0.0174=6.8B | 0.0175=3.603 | 0.0172=6.097 |
| | | HVL (mm) | 40.77 | 41.01 | 39.83 | 39.60 | 40.29 |
| | | Mfp (mm) | 5B.B2 | 59.17 | 57.47 | 57.14 | 5B.13 |
| | | Hardness test | 33 | 36 | 34 | 29 | 30 |
| | Set3 Steel slices | $\bar{\mu}$ (mm$^{-1}$) & $\sigma(\bar{\mu})\times10^{-3}$ | 0.0163=4.97 | 0.0167=2.64 | 0.0170=2.84 | 0.0173=7.926 | 0.0171=4.3B7 |
| | | HVL (mm) | 42.52 | 41.50 | 40.77 | 3B.72 | 40.53 |
| | | Mfp (mm) | 61.34 | 59.BB | 5B.B2 | 55.B6 | 5B.47 |
| | | Hardness test | 40 | 43 | 46 | 50 | 55 |

**Table 5**
AVERAGE LINER ATTENUATION COEFFICIENT (mm$^{-1}$)WITH THE STANDARD DEVIATION, HVL, HARDNESS AND mfp FOR THE TESTED SAMPLES FOR $^{60}$Co(1.33MeV).

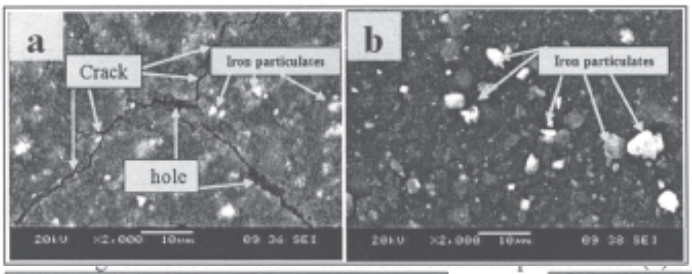


Fig. 8. Rubber matrix with additive of iron particulates (a) 75%wt. (b) 65%wt.

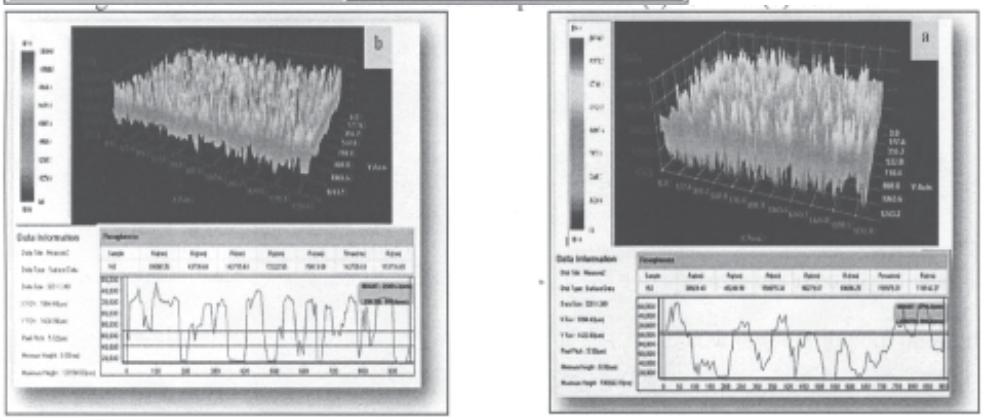

Fig. 9. Three-D surface scanning analyses for samples containing iron particulate addition (a) 65 wt.%, (b) 75 wt.%.

The value of the linear attenuation coefficient for the fabricated samples was increased as the additives increase; particularly for samples No.4which contains 65 wt. %additives. In fact, sample 4 produced attenuation of 13% more than other samples at energy of 0.662 MeV for $^{137}$Cs radioactive source. SampleNo.5 contained 75wt. % additives showed inferior performance against radiation. This because increasing additives content leads to cracks and holes formation. This is clearly demonstrated in figure .8.These cracks and/or holes reduce the cohesiveness of the rubber matrix and deteriorates its homogeneity. On the other hand, increased additions over the acceptable threshold leads to loss rubber many of its properties, these leads to unsatisfying result of attenuation coefficient, these cracks and holes and rough surfaces could be due to matrix degradation. In addition, surface cracks can be formed by increasing the ratio of additives from 75%wt and up. Figure 9 shows Three-dimensional surface scanning analyses for a sample contents iron particulate (a) of 65 wt. % and (b) of 75 wt.%. It is evident that the sample with 75 wt. % additives has a rough surface, non-homogeneous and includes many deep pores as compared to that of 65 wt. % additives. This proves that there is a threshold value for particulates content and if this value is surpassed the mechanical properties and shape retaining of the samples will be enormously affected. This value is particulate's shape and size dependant, in this study the threshold value has ranged between 65 to 75 wt. %.

Figures 10,11,12 Describe the behaviour of the linear attenuation coefficient with the Additives content for $^{137}$Cs energy level 0.662MeV and for the two energy levels of $^{60}$Co 1.17 and 1.33 MeV. It is clearly evident from Fig. 10 that generally increasing the additives content leads to a higher linear attenuation coefficient, samples of iron particles in set1 showed tremendous effect of the additive content on $\mu$. After a certain threshold value increasing the iron particulates content diminish the attenuation coefficient value. This threshold point indicates the collapse and the loss of rubber to its properties.

For comparison purposes the value of $\mu$ for the rubber mix as a matrix without any additives was measured for three energy levels 0.662, 1.17 and 1.33 MeV to be of 0.0162, 0.0137 and 0.0102 mm$^{-1}$ respectively. These values are less than the values of $\mu$ with additives. This clearly reveals the

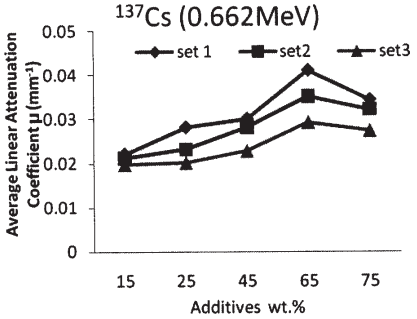


Fig. 10. The average linear attenuation coefficient ($\mu$)with mixing ratios for $^{137}$Cs source of 0.662MeV energy level, Set 1, 2 and 3 are for iron particulates, powder iron filling, and powder Steel slags additions respectively.

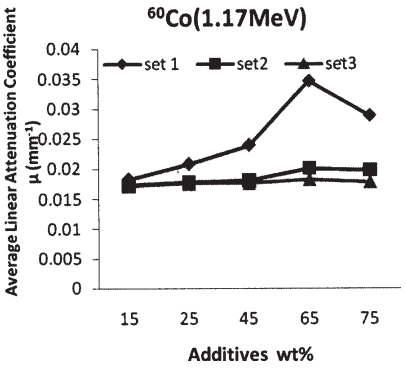


Fig. 11. The average linear attenuation coefficient vs. mixing ratio for $^{60}$Co source of 1.17MeV energy level

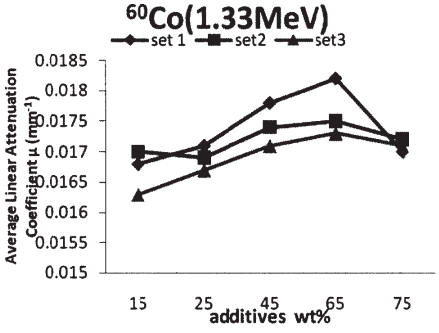


Fig. 12. The average linear attenuation coefficient against additives content for $^{60}$Co source of 1.33MeV energy level.

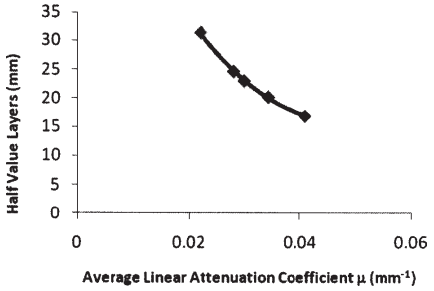


Fig. 13. The HVL vs. the average linear attenuation coefficient for the samples of iron particulates at 0.662 MeV.

**Table 6**
COMPARISON BETWEEN DIFFERENT SHIELDING MATERIALS FOR ATTENUATION OF GAMMA-RAYS AT ENERGY LEVEL OF 0.66 MeV.

| Thickness X(mm) | | | | | Shield |
|---|---|---|---|---|---|
| 99.90% | 90% | 50% | 20% | μ (1/mm) | |
| 42.64 | 21.32 | 6.42 | 2.07 | 0.108 | Lead [35 ] |
| 94.69 | 41.25 | 12.83 | 3.75 | 0.0410 | Sample 4, present work |
| 163.3 | 81.65 | 24.57 | 7.91 | 0.0282 | 70%BaO-10%$B_2O_3$-20%Flyash glass [36] |
| 183.47 | 91.7 | 27.61 | 8.89 | 0.0251 | Barite concrete [37] |
| 197.6 | 98.82 | 29.7 | 9.58 | 0.0233 | Special Lead Glass [38] |
| 214.19 | 107.1 | 32.23 | 10.37 | 0.0215 | (80-x)$B_2O_3$-10Al2$O_3$-10$SiO_2$-x$CaF_2$ (where x = 5,10,20,25,30,35and 40) glass system [39] |
| 273.3 | 136.6 | 41.1 | 13.24 | 0.0168 | Concrete (white sand) [27] |
| 307.01 | 153.5 | 46.2 | 14.87 | 0.015 | Diorite rock [40] |
| 365.5 | 182.7 | 5.5 | 17.7 | 0.0126 | Compressed soil [41] |
| 1096.5 | 548.2 | 165 | 53.12 | 0.0042 | Water [35] |

effect of metal particulates addition on the protection level. Figure 13 showed the half values layers with the average linear attenuation coefficient for the samples with iron particulates at 0.662 MeV.

The dependence in figures 10-11-12 and 13 can be explained using the following formulae [34].

$$\sigma_{ph} \approx \frac{KZ^5}{E^{3.5}} \quad (5)$$

where: $\sigma_{ph}$ is the photoelectric cross-section this relation is valid for gamma-ray energies of few hundreds of keV, knowing that;

$$\mu = N\sigma_{ph} \quad (6)$$

where: N is the atomic density.

The thickness, in this study, was determined in order to attain a certain extent of gamma attenuation (0.662 MeV) for different kinds of defense shields. For detailed results, see table 6. From the results mentioned in table 6, it can be deduced that there is an inverse relation between linear coefficient and thickness of shields. For example, in order to attenuate half of the incident gamma rays, variation in HVL values was required, which is also indicated in table 6. The results show that the 4th sample was found to be the most effective one because it contained large quantity of fine iron particles; apart from pure lead, this combination was found to be a very effective defense shield. Tables 6 also shows that HVL and sample density have an inverse relation, which can be seen more clearly in figure 13.

Figure 14 shows the behaviour of μ with the different energy levels used; it clearly shows that as the energy increases the value of μ decreases.

Figure 15 showed that hardness of the samples incorporated slags is higher than that of iron fillings and iron particulate. This might be attributed to the evenly distributed small particle size of slags as compared to the other particulates and to the higher volume fraction of slags within the rubber matrix.

*Fourier Transform Infrared (FTIR) Spectroscopy*

Figure 16 shows FTIR spectra for different particulate rubber-particulate samples. Peaks at 3355, 3275 and 3320 $cm^{-1}$ corresponds to intermolecular hydrogen bonding of iron filling, particulate and steel slags addition respectively [42]. This proves that the intermolecular hydrogen bonding is a polymeric structure of NBRr and NR. However the number of interaction is limited due to abundance of hydrogen atom and less of nitrogen atom in the structure. The peak at 2913 and 2845 $cm^{-1}$ indicate the asymmetric and symmetric –CH2- stretching band of both NR and NBRr. Besides, the C-H characteristics are shown at 1440 and 1374 $cm^{-1}$ in all spectra [42].

The sulfur crosslink is present between NR and NBR and shown via extremely weak peak at region 700 to 590 $cm^{-1}$ [42]. The present of amine group in NBRr stabilized metal particulate via chelating effect as given in the proposed structure figure 17 .

Set 1, 2 and 3 are for Iron particulates, powder Iron filling, and steel slags addition respectively.

Figure 18 shows the density against additives wt. %. It is clearly evident that the samples density is related to the additives rate, increasing the content of the heavier component within the composite results in higher overall density of the composite.

*Density measurements*

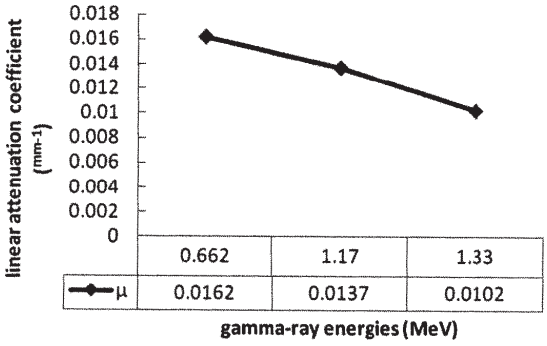


Fig. 14. The linear attenuation coefficient of rubber mix (matrix) without any particulates additions against different gamma-ray energies.

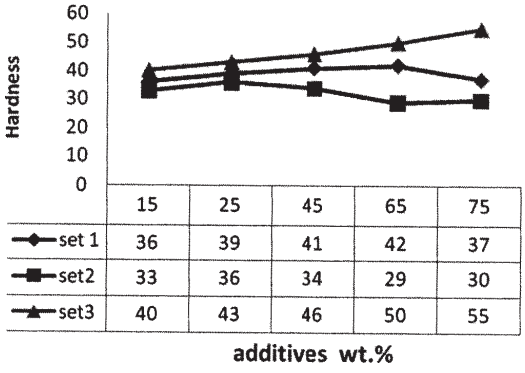


Fig. 15. The hardness value against wt. % of different particulates.

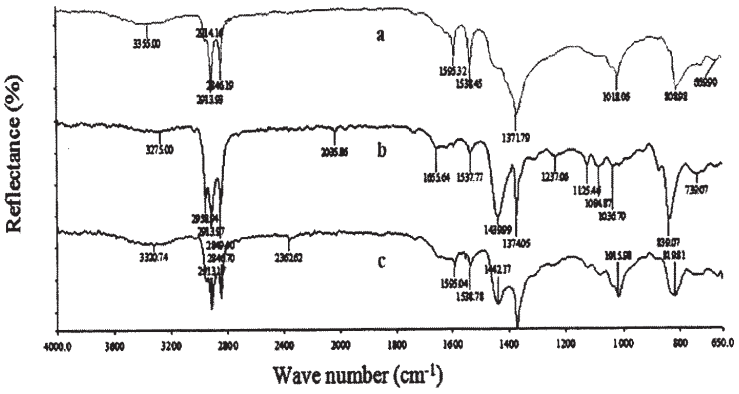


Fig. 16. IR spectrum for different rubber–particulate samples (a)65wt. % iron fillings addition,(b)65wt. % iron particulates addition(c)65wt. % steel slags addition

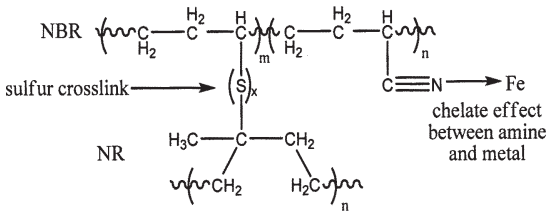


Fig. 17. Propose structure of amine group in NBRr stabilized metal particulate via chelating effect

The density for natural rubber without any addition was calculated by direct dimensions measurement from the weight of the rubber chunks divided by their volumes.

$$\rho = \frac{m}{v} \qquad \rho_{pure} = 1.277\ {}^{g}/_{cm^3} \tag{7}$$

The prediction of theoretical density (TD) for a mixture of three materials or a powder and a binder requires some analysis. Suppose the theoretical density of the three materials to be designated as $v_{Al}$, $\rho_{rubber}$ and $\rho_{iron.}$ The density of the mixture is given by dividing the total mass by the total volume. The total mass $W_T$ is:

$$W_T = W_{Al} + W_{Rubber} + W_{Iron} \tag{8}$$

The volume of each material is the mass divided by the density,

$$V_{Al} = \frac{W_{Al}}{\rho_{Al}} \qquad V_R = \frac{W_R}{\rho_R} \qquad V_i = \frac{W_i}{\rho_i}$$

Thus the total volume $V_T$ is given as the sum of the volumes of the three materials $V_{Al} + V_R + V_i$. Hence the theoretical density for the mixture $\rho_T$ is given as the total weight divided by the total volume.

$$\rho_T = \frac{W_T}{V_T} = \frac{W_{Al-mesh} + W_{rubber} + W_{iron}}{\left[\left(\frac{W_{Al-mesh}}{\rho_{Al}}\right) + \left(\frac{W_{rubber}}{\rho_{rubber}}\right) + \left(\frac{W_{iron}}{\rho_{iron}}\right)\right]} \tag{9}$$

$\rho_T$ is the theoretical density.
$\rho_T = 1.59\ g/cm^3$

Now if a rule of mixture is applied in estimating the theoretical density for a mixture, a considerable error will be encountered. As an example, for rubber mixture of NR/NBRr, iron particulates 65wt.% and aluminum mesh ; the theoretical density according to the above expressions is $1.597\ g/cm^3$ while following the rule of mixture gives TD of $1.277\ g/cm^3$.

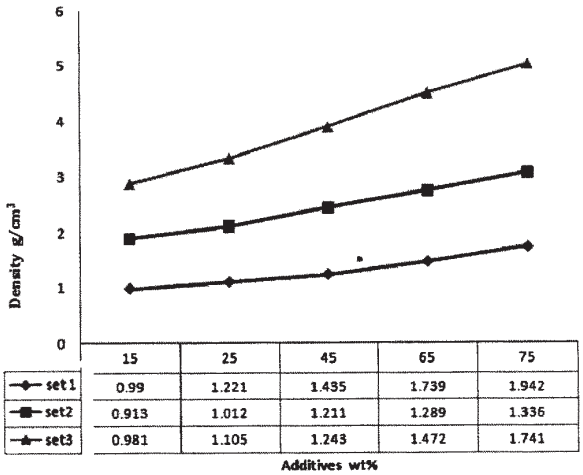


| | 15 | 25 | 45 | 65 | 75 |
|---|---|---|---|---|---|
| set1 | 0.99 | 1.221 | 1.435 | 1.739 | 1.942 |
| set2 | 0.913 | 1.012 | 1.211 | 1.289 | 1.336 |
| set3 | 0.981 | 1.105 | 1.243 | 1.472 | 1.741 |

Fig. 18. Samples density versus wt.% of additives

The results are also confirmed by previous research [43-48], opening new fields of interest in the radiation shielding materials study.

## Conclusions

The mixture of NR/NBRr was found to be the most appropriate formula for synthesizing light weight and high density rubber shield against radioactive radiations and high speed neutrons. The mixture generated better results than the traditional lead shields which are currently being used in radiotherapy industry.

A mixture of rubber blends and pure iron particles can improve the shielding properties of rubber and makes rubber a good absorbent for radioactive radiations.

The mixture can be used in medical units, nuclear stations, storage houses to prevent gamma rays and other radioactive particles from escaping into the environment, coating the walls and roofs of storage houses by this mixture can significantly reduce the risk.

In order to make the manufacturing procedure cost effective and environment friendly, waste rubber can be used with natural rubber to increase the thickness and density of the shield.

The samples prepared were found to be flexible and had high compressive strength. The homogenous composition made the samples impact proof.

$\mu$ and radiation energy are inversely proportional to each other while $\mu$ and mixing ratios are directly proportional to each other.

HVLS and $\mu$ are inversely proportional to each other.

## References

1.PEREZ, J. M., VILAS, J. L., LAZA, J. M., ARNA´IZ, S., MIJANGOS, F., BILBAO, E., RODRI´GUEZ, M., LEO´N, L. M. Journal Material Process Technology **210**, 2010, 727.
2.ANANDHAN, S., DE, P.P., BHOWMICK, A.K., BANDYOPADHYAY, S., DE, S.K., J. Applied Polymer Science **90**, 2003, p. 2348.
3.AKKURT, I., MAVI, B., AKKURT, A., BASYIGIT, C., KILINCARSLAN, S., YALIM H., J. Quant. Spectrosc. Radiat. Transf. **94**, 2005, p. 379.
4.SCUDERI, G.J., BRUSOVANIK, G.V., CAMPBELL, D.R., HENRY, R.P., KWON, B., VACCARO, A.R.. Spine J., **6**(5), 2006, p. 577.
5.NGAILE, J.E., UISO, C.B., MSAKI, P., KAZEMA, R., Radiate Prot Dosimeter. **130**(4), 2008, p. 490.
6.MCGINLEY, P.H., MINER, M.S., Health Phys. **69**(5), 1995, p. 759.
7.HULBERT, S.M., CARLSON, K.A., J. Nucl Med Technol. **37**(3), 2009, p. 170.

8.VERSTRAETEN, S.V., AIMO, L., OTEIZA, P.I., Arch Toxicol. **82**(11), 2008, p. 789.
9.COON, T., MILLER, M., SHIRAZI, F., SULLIVAN, J., Pediatrics., **117**(1), 2006, p. 227.
10.HEALEY, N., Radiat Prot Dosimetry, **134**(3-4), 2009, p. 143.
11.HEATH, L.M., SOOLE, K.L., MCLAUGHLIN, M.L., MCEWAN, G.T., EDWARDS, J.W., Rev Environ Health. **18**(4), 2003, p. 231.
12.MILLSTONE, E., RUSSELL, J., J. R. Soc Health. **115**(6), 1995, p. 347.
13.MURATA, K., IWATA, T., DAKEISHI, M., KARITA, K., J Occup Health, **51**(1), 2009, p. 1.
14.VIG, E.K., HU, H., J Am Geriatr Soc., **48**(11), 2000, p. 1501.
15.SCHICK, D.K., CASEY, R.N., SIM, L.H., SIDDLE, K.J. Australas Radiol. **43**(1), 1999, p. 47.
16.RAMMAH, S., AL-HENT, R., YOUSEF, S., Availability of Special Local Rock Materials for Using in Radiation Shielding Concrete. (Atomic Energy Commission of Syria) A.E.C.S. 2003, p. 33.
17.JAEGER, R.G., BLIZARD, E.P., CHILTON, A.B., GROTENHUIS, M., HOENIG, A., JAEGER, T.A., Engineering Compendium on Radiation Shielding. In Shielding Materials; Springer-Verlag: vol.2, 1975.
18.MCCAFFREY, J.P., SHEN, H., DOWNTON, B., MAINEGRA-HING, E., Med. Phys., **34**, 2007, p. 530.
19.EDER, H., SCHLATTL, H., HOESCHEN, C., Rofo. **182**(5), 2010, p. 422.
20.JOHNS, H.E., CUNNINGHAM, J.R., The Physics of Radiology, (1978) 3rdedn.
21.SHAPIRO, J., Radiation protection: a guide for scientists and physicians, (1982) 2ndedn.
22.HILL, A., Br J Radiol **72**(860), 1999, p. 792.
23.HUSSAIN, R., HAQ, Z., MOHAMMAD, D., J Islamic Acad Sci **10**(3), 1997 p. 81.
24.FUGA, P., J Radioanal Nucl Chem **149**(2), 1990, p. 287.
25.BRAOUDAKIS, G., Nucl Instrum Methods, **403**, 1998, p. 449.
26.MURBUT, A., NAMAH, A., TAKI, A., Sci J Iraqi at Energy Comm **2**(2), 2000, p. 46.
27.JAMEEL, H., AL-DAYEL, O., AL-HORAYESS, O., AL- AJYAN. Energy Power Eng., **2**, 2010, p. 6.
28.MAHEEMEED, A.K., HASAN, H.I., AL-JOMAILY, F.M., J. Radioanal. Nucl. Chem., **291**, 2012, p. 653.
29.AGHAMIRI, M.R., MORTAZAVI, S.M.J., TAYEBI, M., MOSLEH-SHIRAZI, M.A., BAHARVAND, H., TAVAKKOLI-GOLPAYEGANI, A., ZEINALI-AFSANJANI, B., J Biomed Phys Eng., **1**(1), 2011.
30.NORIMAN, N.Z., ISMAIL, H., RASHID, A., Polym Plast Technol Eng, **47**, 2008, p. 1.
31.FLORY, P.J., REHNER, J., Journal Chem Phys, **11**, 1943, p. 512.
32.AKKURT, I., CANAKCI, H., Iran. J. Radiat. Res. **9**, 2011, p. 37.
33.ISMAIL, Z.Z., AL-HASHMI, E.A., Waste Manag., **28**, 2008, p. 2048.
34.LILLEY, J., Nuclear physics principles and application. Wiley, University of Manchester, New York, 2001.
35.AL-AHMED, K.O., Introduction of health physics. Dar-Al Ktub for printing and Publishing University of Mosul. Press Mosul University, Mosul, 1993.
36.SUPARAT, T., JAKRAPONG, K., PICHET, L., WEERAPONG, C., Nucl Sci Technol 1, 2011, p. 110.
37.STANKOVIC, S., ILIC, R., JANKOVIC, K., BOJOVIC, D., LONCAR, B.X., Acta Phys Polonica A **117**(5), 1993, p. 812.
38.FATHI, F., Raf J Sci **17**(2), 2005, p. 130.
39.EL-SERSY, A., HUSSEIN, A., EL-SEMMAN, H., EL-ADAWY, A., DONYA, H., J Radioanal Nucl Chem **288**, 2011, p. 65.
40.EL-TAHER, A., Indian J. Pure Applied Physics **45,** 2007, p. 198.
41.MURBUT, A., NAMAH, A., TAKI, A., Sci J Iraqi at Energy Comm **2**(2), 2000, p. 46.
42.CONLEY, R.T., Infrared Spectroscopy, 2nd Edition, Boston: Allyn and Bacon Inc. 1972,
43.AZEEZ, A.B., MOHAMMED, K.S., SANDU, A.V., AL BAKRI, A.M.M., KAMARUDIN, H., SANDU, I.G., Rev. Chim. (Bucharest), **64**, no. 8, 2013, p. 899.
44.RAZAK, R.A., ABDULLAH, M.M.A., KAMARUDIN, H., ISMAIL, K.N., SANDU, I., HARDJITO, D., YAHYA, Z., Rev. Chim. (Bucharest), **64**, no. 6, 2013, p. 593.
45.TABACARU, C., CARLESCU, A., SANDU, A.V., PETCU, M.I., IACOMI, F., Rev. Chim. (Bucharest), **62**, no. 4, 2011, p. 427.
46.AL BAKRI, A.M.M., KAMARUDIN, H., NIZAR, I.K., SANDU, A.V., BINHUSSAIN, M., ZARINA, Y., RAFIZA, A.R., Rev. Chim. (Bucharest), **64**, no. 4, 2013, p. 382.
47.YAHYA, Z., ABDULLAH, M.M.A., HUSSIN, K., ISMAIL, K.N., SANDU, A.V., VIZUREANU, P., ABD RAZAK, R., Rev. Chim. (Bucharest), **64**, no. 12, 2013, p. 1408.
48.IZZAT, A.M., AL BAKRI, A.M.M., KAMARUDIN, H., SANDU, A.V., RUZAIDI, G.C.M., FAHEEM, M.T.M., MOGA, L.M., Rev. Chim. (Bucharest), **64**, no. 9, 2013, p. 1011

Manuscript received: 18.08.2014